

1 **Migratory divides coincide with species barriers across replicated avian hybrid zones**
2 **above the Tibetan Plateau**

3

4 Elizabeth S.C. Scordato^{1,2*}, Chris C.R. Smith¹, Georgy A. Semenov^{1,3}, Yu Liu^{4,5}, Matthew R.
5 Wilkins^{1,6}, Wei Liang⁷, Alexander Rubtsov⁸, Gomboobaatar Sundev^{9,10}, Kazuo Koyama¹¹,
6 Sheela P. Turbek¹, Michael B. Wunder¹², Craig A. Stricker¹³, Rebecca J. Safran¹

7

8 1. Department of Ecology and Evolutionary Biology, The University of Colorado, Boulder, CO,
9 USA

10 2. Department of Biological Sciences, California State Polytechnic University, Pomona, CA,
11 USA

12 3. Institute of Ecology and Systematics of Animals, Novosibirsk, Russia

13 4. Queen Mary University of London, London, England

14 5. Beijing Normal University, Beijing, China

15 6. Vanderbilt University, Center for Science Outreach, Nashville, TN 37212

16 7. Ministry of Education Key Laboratory for Ecology of Tropical Islands, College of Life
17 Sciences, Hainan Normal University, Haikou 571158, China

18

19 8. State Darwin Museum, Moscow, 117292 Russia,

20

21 9. National University of Mongolia P. O. Box 537, Ulaanbaatar 210646, Mongolia

22 10. Mongolian Ornithological Society, P. O. Box 537, Ulaanbaatar 210646, Mongolia

23 11. Japan Bird Research Association, Tokyo, Japan 183-0034

24 12. Department of Integrative Biology, University of Colorado Denver, Denver, CO USA

25 13. United States Geological Survey, Denver Federal Center, Denver, CO 80225

26

27 **Keywords:** migratory divide, hybrid zone, reproductive isolation, speciation, barn swallow

28 **Short title:** Reproductive isolation at migratory divides

29

30 * Corresponding author:

31 Elizabeth Scordato

32 Department of Biological Sciences

33 Cal Poly Pomona

34 Pomona, CA, 91768

35 escordato@cpp.edu

36

37

38

39 **Author contributions**

40 ESCS and RJS conceived of the study. ESCS carried out the fieldwork, with assistance from GS,

41 YL, MRW, WL, AR, GS, and KK. CCR did the sequence alignments and variant calling. CS

42 processed the stable isotope data. ESCS analyzed the data with input from CCR, MRW, MBW

43 and RJS. ESCS wrote the manuscript with input from all authors, especially ST and RJS.

44

45

46 **Abstract**

47 Migratory divides are proposed to be catalysts for speciation across a diversity of taxa. However,
48 the relative contribution of migratory behavior to reproductive isolation is difficult to test.
49 Comparing reproductive isolation in hybrid zones with and without migratory divides offers a
50 rare opportunity to directly examine the contribution of divergent migratory behavior to
51 reproductive barriers. We show that across replicate sampling transects of two pairs of barn
52 swallow (*Hirundo rustica*) subspecies, strong reproductive isolation coincided with an apparent
53 migratory divide spanning 20 degrees of latitude. A third subspecies pair exhibited no evidence
54 for a migratory divide and hybridized extensively. Within migratory divides, migratory
55 phenotype was associated with assortative mating, implicating a central contribution of divergent
56 migratory behavior to reproductive barriers. The remarkable geographic coincidence between
57 migratory divides and genetic breaks supports a longstanding hypothesis that the Tibetan Plateau
58 is a substantial barrier contributing to the diversity of Siberian avifauna.

59

60 **Introduction**

61 Migratory divides- regions where sympatric breeding populations overwinter in different
62 geographic locations- have been proposed to facilitate completion of the speciation process by
63 generating reproductive barriers that maintain species boundaries. Migratory divides can lead to
64 prezygotic reproductive barriers via assortative mating if individuals with different wintering
65 grounds arrive to breed at different times (Bearhop *et al.* 2005; Rolshausen *et al.* 2009; Taylor &
66 Friesen 2017). They can also accelerate the evolution of postmating barriers if hybrids incur
67 survival costs associated with the use of maladaptive routes between breeding and nonbreeding
68 locations (Helbig 1991, 1996; Berthold *et al.* 1992; Delmore & Irwin 2014; Lundberg *et al.*
69 2017). However, establishing a clear link between divergent migratory behavior and
70 reproductive isolation has been challenging. Migratory divides often occur at hybrid zones or
71 regions of secondary contact, where evolutionary history, divergence in traits unrelated to
72 migratory behavior, and ecological differences can also contribute to reproductive barriers
73 (Ruegg 2008; Ruegg *et al.* 2012; Delmore *et al.* 2016; Toews *et al.* 2017). Isolating the effects of
74 migratory behavior on reproductive barriers is particularly challenging when a single region of
75 contact is examined between taxa with broad geographic distributions, because it is not possible
76 to assess the generality of divergent migratory behavior in restricting gene flow across the
77 species range. We therefore lack a comprehensive understanding of the relative importance of
78 divergent migratory behavior to the formation and maintenance of species boundaries (Turbek *et*
79 *al.* 2018).

80 Here we evaluate the hypothesis that migratory divides play a central role in the
81 maintenance of reproductive isolation in secondary contact. We specifically examine three
82 predictions of this hypothesis. First, hybridization should be more limited in contact zones with

83 migratory divides compared to contact zones without migratory divides, when controlling for
84 evolutionary history and divergence in non-migratory traits. Second, if migratory divides *per se*
85 limit hybridization, migratory phenotype should explain a larger proportion of genetic variance
86 among individuals than other divergent traits within migratory divides. Third, if migratory
87 divides act as important premating reproductive barriers, then assortative mating by migratory
88 phenotype should be stronger than assortative mating based on other divergent traits. Previous
89 studies have found mixed evidence for assortative mating and genetic differentiation at migratory
90 divides (Turbek *et al.* 2018), but have not assessed the relative contributions of different traits to
91 reproductive barriers or compared reproductive isolation in hybrid zones with and without
92 migratory divides. We evaluate these predictions in three subspecies of barn swallow (*Hirundo*
93 *rustica*) that hybridize in Asia.

94 Barn swallows comprise six subspecies, of which three (*H. r. rustica*, *H. r. tytleri*, and *H.*
95 *r. gutturalis*) are long-distance migrants that diverged in allopatry (Zink *et al.* 2006; Dor *et al.*
96 2010) but now share breeding range boundaries in Siberia and central Asia (Scordato & Safran
97 2014). There is a narrow hybrid zone in central Siberia between *rustica* and *tytleri*, but extensive
98 hybridization in eastern Siberia between *tytleri* and *gutturalis* (Scordato *et al.* 2017, Figure 1).
99 Differentiation in mtDNA is shallow and indicates that *gutturalis* and *tytleri* are more closely
100 related to one another than either is to *rustica* (Zink *et al.* 2006; Dor *et al.* 2010), but genome-
101 wide pairwise F_{ST} is similarly small (~ 0.02) among allopatric populations of all three subspecies
102 (Scordato *et al.* 2017). There is thus dramatic variation in the strength of reproductive isolation
103 between subspecies, despite similarly shallow genetic differentiation.

104 We evaluated the extent to which a migratory divide explains this variation in strength of
105 reproductive isolation. The geographic location of the narrow hybrid zone in Siberia coincides

106 with reported migratory divides in several other pairs of avian taxa (Irwin & Irwin 2005). The
107 convergence of migratory divides in this region may be caused by the Tibetan Plateau: small-
108 bodied passerines tend to migrate to the west or east around this geographic barrier (Irwin &
109 Irwin 2005). Divergent migratory behavior has therefore been proposed to be broadly important
110 to the evolution and maintenance of species boundaries in Siberian avifauna (Irwin & Irwin
111 2005). However, barn swallow subspecies also differ in ventral plumage coloration, tail streamer
112 length, and body size (Turner 2010; Scordato & Safran 2014), and these traits could be more
113 important reproductive barriers than migratory behavior. We quantified the relative contribution
114 of migratory behavior to reproductive barriers via comprehensive measurement of phenotype,
115 detailed genomic analyses, and measures of assortative mating. We applied these measures to
116 replicated transects to assess the generality of our results across a large proportion of the species
117 range.

118

119 **Materials and Methods**

120 *Sampling*

121 We sampled 1288 birds across the range boundaries of the three Eurasian barn swallow
122 subspecies (Figures 1, 2). In addition to previously sampled hybrid zones between *rustica-tytleri*
123 and *tytleri-gutturalis* in Russia (Scordato *et al.* 2017), we discovered a hybrid zone between
124 *rustica* and *gutturalis* in western China, as well as additional regions of contact between *tytleri-*
125 *gutturalis* and *rustica-tytleri* in Mongolia and China (Figures 1, 2).

126 Sampling was conducted during barn swallow breeding seasons (April-July 2013 in
127 Russia, April-July 2014 in China, Mongolia, and Japan, and May-June 2015 in western China).
128 Birds were caught in mist nets and individually banded with numbered aluminum leg bands. An

129 ~80ul blood sample was collected via brachial venipuncture and stored in Queen's lysis buffer.
130 We collected 5-10 feathers from the throat, breast, belly, and vent of each bird for quantification
131 of color, and collected the inner two tail rectrices for analysis of stable isotopes. Length of the
132 right wing chord, tail streamers, and each primary feather were measured to the nearest 0.1mm,
133 and weight was measured to 0.5g. Each morphometric measurement was taken 3 times per bird,
134 and averaged measurements were used in subsequent analyses. The length of the primary
135 feathers was used to calculate wing pointedness and convexity (Lockwood *et al.* 1998). Wing
136 length has been used as a proxy for migratory distance (Safran *et al.* 2016), but is also correlated
137 with body size, whereas wing shape (pointedness and convexity) has been explicitly linked to
138 migratory distance and is independent of body size (Lockwood *et al.* 1998).

139

140 *Social pair identification*

141 Barn swallows are socially monogamous, with both males and females building the nest and
142 provisioning offspring (Turner 2010). To assess assortative mating, we assigned birds to a social
143 pair if the male and female were unambiguously caught at the same nest. It was not possible to
144 assign birds to pairs in large colonies because they were not caught at individual nests. Our
145 measures of assortative mating are therefore derived from birds nesting singly or in small groups.

146

147 *Quantification of color, identification of variants*

148 We analyzed plumage color using a spectrophotometer. DNA was extracted and sequenced on
149 four replicate Illumina HiSeq lanes. Reads were aligned to a draft barn swallow reference
150 genome (Safran *et al.* 2016) and variants called using *bcftools* and *samtools* (Li & Durbin 2009;
151 Li *et al.* 2009). We identified 12,383 single nucleotide polymorphisms (SNPs) with 5% minor

152 allele frequency cutoff and median read depth of seven reads per locus. Methods for color
153 quantification, sequencing, and variant calling are described elsewhere (Safran & McGraw 2004;
154 Hubbard *et al.* 2015; Safran *et al.* 2016; Scordato *et al.* 2017; Smith *et al.* 2018) and are detailed
155 in the Supplemental Material.

156

157 **Analysis**

158 ***Evidence for a migratory divide***

159 We assessed evidence for migratory divides by analyzing stable carbon ($\delta^{13}\text{C}$) values in tail
160 feathers collected from birds on the breeding grounds (see Supplemental Material). Barn
161 swallows molt their tail feathers in the winter (Turner 2010). Because feather keratin is
162 metabolically inert after formation, feathers sampled during the summer reflect isotopic
163 environments occupied during winter, when feathers were grown. Stable isotope values do not
164 provide direct information about geographic locations of feather growth. However,
165 environmental $\delta^{13}\text{C}$ values vary systematically and widely with water use efficiency of plants;
166 this differentiation is preserved through the food web to animals, such that large differences in
167 feather $\delta^{13}\text{C}$ between individuals suggest those individuals grew their feathers in different
168 environments (Kelly 2000). We evaluated differences in the distribution of $\delta^{13}\text{C}$ values between
169 each of the three subspecies and among hybrids in regions of secondary contact. We found
170 support for migratory divides between *rustica-tytleri* and *rustica-gutturialis* (see Results, Figures
171 1, 2). We use $\delta^{13}\text{C}$ values (hereafter “carbon isotope values”) as proxies for an individual’s
172 migratory phenotype in subsequent analysis.

173

174 ***Prediction one: population structure and extent of hybridization***

175 *Population structure:* We used three complementary methods to analyze population structure:
176 principal components analysis (PCA), which does not require an *a priori* number of populations;
177 TESS (Caye *et al.* 2016), a spatially explicit clustering method that assigns individuals to *K*
178 clusters but weights individual admixture proportions by geographic proximity; and
179 fastSTRUCTURE (Raj *et al.* 2014), which uses a variational Bayesian algorithm to assign
180 individuals to *K* clusters without weighting by geographic proximity. We ran the PCA on the
181 genome-wide covariance matrix of 12,383 SNPs across 1288 individuals using the R function
182 *prcomp*. We ran TESS on the same set of SNPs for values of *K* from 2-5, with 3 repetitions per
183 *K*, 1000 iterations, and the regularization parameter (α)= 0.001. This regularization value
184 does not weight geographic location particularly strongly in the analysis (Caye *et al.* 2016). We
185 ran the fastSTRUCTURE model with the “simple” prior for values of *K* from 1-15 and a cross-
186 validation of 5 repetitions per *K*. In fastSTRUCTURE, the best value of *K* is the minimum
187 number of model components (*K*) that explain 99.99% of the admixture in the sample.(Raj *et al.*
188 2014) We found *K*=3 to be the best value. We assigned individual birds to hybrid classes (F1,
189 later generation hybrid, or backcross) by calculating hybrid indices and average heterozygosity
190 across subsets of differentiated loci using the R package *introgress* (Supplemental Material).
191
192 *Geographic cline analysis:* To determine whether geographic variation in the frequency of
193 hybridization coincides with differences in migratory behavior or other divergent phenotypic
194 traits, we fit sigmoidal geographic clines (Szymura & Barton 1986) to three east-west transects
195 spanning contact zones between *rustica-tytleri* (two transects) and *rustica-gutturalis* (one
196 transect, Figure 1). Transects spanned 85-115 degrees longitude. We explicitly compared the
197 extent of hybridization in regions with and without putative migratory divides by fitting clines to

198 three parallel transects at the same latitudes but farther-eastern longitudes (106-140 degrees)
199 through regions of admixture between *tyleri* and *gutturalis* (Figure 1). Clines were fit to
200 genomic ancestry, measured as PC1 from the PCA of the genome-wide covariance matrix. PC1
201 explained 30% of the genetic variance and clearly separated the three subspecies as well as
202 hybrids (Figure 2). To assess whether variation in phenotype was geographically concordant
203 with admixture, we also fit clines to breast chroma, throat chroma, carbon isotope value, tail
204 streamer length, wing convexity, wing pointedness, and wing length. Cline analysis was
205 implemented in the R package HZAR (Derryberry *et al.* 2014, Supplemental Material). We
206 applied neutral diffusion equations (Barton & Gale 1993) to determine whether cline widths
207 were narrower than expected under a scenario of no selection or reproductive isolation, assuming
208 a one-year generation time and dispersal distances of 42km (conservative) or 100km (less
209 conservative, Paradis *et al.* 1998; Supplemental Material). Cline widths narrower than the neutral
210 expectation may be maintained by selection and contribute to reproductive barriers (Ruegg 2008;
211 Brelsford & Irwin 2009). Concordant clines between ancestry and phenotypic traits may indicate
212 that those traits are associated with reproductive barriers (Gay *et al.* 2008; Gompert & Buerkle
213 2016).

214

215 ***Prediction two: variance partitioning***

216 To test the prediction that traits associated with reproductive barriers explain comparatively large
217 proportions of genetic variance, we partitioned genetic variance among groups of traits using
218 variance partitioning and redundancy analysis in the *ecodist* and *vegan* packages in R (Goslee &
219 Urban 2007; Oksanen *et al.* 2013). This approach determines the amount of variance in a set of
220 response variables that is due to a set of explanatory variables, while conditioning on other sets

221 of variables. It is ideal for large datasets with intercorrelated explanatory variables (Wang 2013;
222 Safran *et al.* 2016). We quantified the amount of variance in genomic PC1 and PC2 (Figure 2)
223 that could be explained by the individual and combined contributions of migratory phenotype
224 (carbon isotope value) and ventral coloration. The broad geographic scale of sampling required
225 controlling for possible isolation-by-distance (Shafer & Wolf 2013; Wang 2013). We therefore
226 analyzed each transect separately and conditioned models on sampling location (latitude and
227 longitude).

228

229 ***Prediction three: assortative mating***

230 Premating reproductive isolation is maintained by assortative mating between individuals with
231 similar genotypes (“like mating with like). However, premating isolation is typically measured
232 by assessing assortative mating by phenotype, under the assumption that phenotype is a
233 reasonable proxy for genotype. Interpreting assortative mating is complicated when there is
234 continuous variation in phenotypes and genotypes between interbreeding groups. We therefore
235 measured assortative mating in two ways. First, we used phenotype networks to identify
236 correlations between an individual’s genotype and its mate’s phenotype. This method leverages
237 continuous variation in genotypes and phenotypes to quantify broad patterns of assortative
238 mating across sampling transects. Second, we calculated standardized indices of reproductive
239 isolation within populations to determine the strength of assortative mating based on different
240 traits (genotype, migratory phenotype, and ventral color). These two methods provide
241 complementary views of assortative mating at different geographic scales. We were able to
242 assign birds to social pairs along three sampling transects: the *rustica-tyleri* transect in Russia,

243 the *rustica-gutturalis* transect in China, and the *tytleri-gutturalis* transect in China (Figure 1).

244 Sufficient social pairing data were not available for the other three transects.

245

246 *Assortative mating: phenotype networks*

247 To accommodate continuous variation between parentals and hybrids we used a Partial

248 Correlation and Information Theory (PCIT) approach (Badyaev & Young 2004; Wilkins *et al.*

249 2015) to identify correlations between male and female phenotypes and genotypes. This method

250 was originally developed for analysis of gene co-expression networks (Reverter & Chan 2008)

251 but is applicable to other networks with complex correlation structures (Shizuka & Farine 2016).

252 We began with a matrix of Spearman rank correlations between pairs of males and females.

253 These matrices included genotype (genomic PC1), ventral color, carbon isotope value, and

254 sampling latitude and longitude for each member of a social pair. To identify and remove

255 spurious correlations, we used the *pcit* package in R (Watson-Haigh *et al.* 2009), which uses the

256 Spearman rank correlation matrix to generate a network of partial correlation coefficients. The

257 PCIT algorithm sets a ‘local threshold’ for inclusion of an edge (i.e. the correlation connecting

258 two traits) based on the average ratio of the partial to direct correlation for every trio of traits

259 (“nodes” on the network). The algorithm begins with a network in which every pair of nodes is

260 connected by an edge whose value is the absolute value of the correlation coefficient between the

261 two traits. An edge between two particular nodes is discarded if the direct correlation coefficient

262 is less than the product of the local threshold and the correlations between each node in the focal

263 pair and the third trait in the trio.

264 We visualized assortative mating for each transect as a bipartite network of correlations

265 with two categories of nodes (male and female). Each node represents a different trait, and lines

266 (edges) connect nodes if traits are correlated within mated pairs (e.g. if darker males mate with
267 darker females; Figure 5, gray lines). Analyzing assortative mating along the transects ensured
268 that each network encompassed individuals with parental and admixed genotypes. Including
269 genotype as a node in the network allowed us to determine which aspects of phenotype might be
270 used as reliable proxies of genotype in the context of maintaining subspecies boundaries. These
271 relationships are shown as black lines in Figure 5 connecting an individual's genotype to the
272 phenotype of its social partner. We generated networks using the R package 'qgraph' (Epskamp
273 *et al.* 2012). To facilitate interpretation, we only show correlations between male and female
274 pairs on the networks (as opposed to within-individual trait correlations), but within-individual
275 correlations were included in the PCIT analysis.

276

277 *Assortative mating: strength of premating isolation*

278 To examine fine-scale assortative mating within populations, we analyzed the strength of
279 premating reproductive isolation (RI) following Sobel and Chen (2014). Here, isolation is
280 calculated based on the proportion of heterospecific pairings divided by the sum of conspecific
281 and heterospecific pairings. This method is advantageous because RI is scaled between -1 and 1,
282 with 1 equal to complete assortative mating, 0 equal to random mating, and -1 equal to complete
283 disassortative mating. The isolation index is directly related to gene flow: $RI = 0.5$ means there
284 are 50% fewer heterospecific pairs in the population than expected by chance, whereas $RI = -0.5$
285 means there are 50% more heterospecific pairs than expected by chance.

286 This RI index requires assigning individuals to categories to determine frequencies of
287 con- vs. heterospecific pairings. We assigned each individual as a "parental" or a "hybrid" based
288 on its genotype, its migratory phenotype, and its color. Assignments were made using 1000

289 repetitions of a linear discriminant analysis (see Supplemental Material). We then calculated the
290 strength of RI based on each trait in each population across the three transects.

291 Because genotype frequencies (i.e. the proportions of parentals vs. hybrids) varied
292 between populations, we followed equation 4S4 in Sobel and Chen (2014) and weighted
293 observed con- and heterospecific pairings by the number of such pairings expected under a
294 scenario of random mating, given the distribution of genotypes in the population:

295

$$296 \quad RI = 1 - \frac{2 * \left(\frac{\text{observed heterospecific pairings}}{\text{expected heterospecific pairings}} \right)}{\left(\frac{\text{observed conspecific pairings}}{\text{expected conspecific pairings}} \right) + \left(\frac{\text{observed heterospecific pairings}}{\text{expected heterospecific pairings}} \right)}$$

297

298 To calculate expected pairings, we used the total pool of individuals (not just those for which we
299 had pairing data) and randomly generated social pairs without replacement. We counted the
300 proportions of con and heterospecific pairs from these random draws. We considered pairings
301 between two hybrid individuals to be “conspecific” and pairings between a parental and a hybrid
302 to be “heterospecific;” this will generally underestimate the strength of reproductive isolation.
303 The expected proportions of each type of pairing under a random mating scenario were averaged
304 over 1000 random draws for each population.

305

306 **Results**

307 *Evidence for a migratory divide*

308 The distribution of $\delta^{13}\text{C}$ in feathers for *tyleri* overlapped almost completely with *gutturalis*,
309 whereas the distribution for *rustica* minimally overlapped the distributions for the other two
310 subspecies (Figure 4, Figure S1). More importantly, the $\delta^{13}\text{C}$ values for *rustica* are consistent
311 with comparatively arid environments where food webs are based on C4 plants, whereas the

312 values for *gutturalis* and *tyleri* are consistent with more mesic environments where food webs
313 are based on C3 plants (Kelly 2000). Furthermore, observed $\delta^{13}\text{C}$ values for *rustica* are
314 consistent with values expected for southern and eastern Africa and the Arabian peninsula, a
315 region dominated by C4 plants (Still *et al.* 2003), and an area of extensive sighting records
316 (Sullivan *et al.* 2009; Turner 2010) for this subspecies during winter. By contrast, both $\delta^{13}\text{C}$
317 distributions and sighting records suggest *tyleri* and *gutturalis* overwinter in south and southeast
318 Asia, a wetter region with comparatively more C3 plants (Still *et al.* 2003). Hybrid zones
319 between *rustica* and *tyleri/gutturalis* exhibit intermediate means and large variances in $\delta^{13}\text{C}$
320 values (Figure S1), suggesting sympatry between individuals overwintering in different
321 locations. We interpret these results as evidence for different wintering grounds and consequent
322 migratory divides between *rustica-tyleri* and *rustica-gutturalis* (Figure 1).

323

324 ***Prediction 1: Limited hybridization is associated with divergent migratory phenotypes***

325 We predicted that if migratory divides act as barriers to reproduction, then hybridization should
326 be limited in contact zones with migratory divides compared to contact zones without migratory
327 divides. Furthermore, clines for carbon isotope values, our proxy for differences in overwintering
328 grounds, should be steep and concordant with genetic ancestry clines.

329 *Population structure and gene flow:* We identified three genetic clusters corresponding to the
330 three subspecies, with dramatic variation in the extent of hybridization between subspecies pairs
331 (Figure 1,2). We found narrow hybrid zones between *rustica-tyleri* and *rustica-gutturalis*,
332 whereas *tyleri* and *gutturalis* were admixed over a large region of east Asia (Figures 1, 2).

333 We found F1, later generation hybrid, and backcrossed individuals between all three
334 subspecies pairs, indicating ongoing gene flow (Figure S2). However, there were few recent

335 hybrids between *rustica-tytleri* (1% F1, 13% later generation) and *rustica-gutturalis* (2% F1,
336 18% later generation, Figure S2), consistent with strong isolation between these two subspecies
337 pairs. By contrast, there were many multi-generation hybrids between *tytleri* and *gutturalis* (8%
338 F1 and 53% later generation; Figure S2), consistent with weak reproductive isolation across a
339 broad geographic region that contains few parental individuals and many hybrids. These analyses
340 reveal less hybridization overall between the subspecies pairs with migratory divides (*rustica-*
341 *tytleri*, *rustica-gutturalis*) compared to the pair without a migratory divide (*tytleri-gutturalis*).

342

343 Geographic clines- *rustica* pairs: Clines for genetic ancestry (genetic PC1) were very narrow
344 between *rustica-tytleri* in Russia and *rustica-gutturalis* in China, suggesting these hybrid zones
345 are maintained by selection or are of unrealistically recent origin (<1 year; Figure 1B, D, Table
346 1). A mountain range separated *rustica* and *tytleri* in western Mongolia, and we found no
347 evidence for extant interbreeding across this barrier (Figure 1C, Table 1). Remarkably, the
348 centers of the ancestry clines in all three *rustica* transects occurred at similar longitudes (between
349 98 and 101 degrees), despite spanning over 20 degrees of latitude and comprising different pairs
350 of subspecies (Figure 1A, white arrows). Carbon isotope clines were narrow and concordant with
351 ancestry in all three *rustica* transects (Figure 1, Table 1). The locations of narrow hybrid zones
352 thus coincide with migratory divides.

353 Ventral coloration also varied among *rustica* pairs. A narrow ventral color cline in Russia
354 coincided with the ancestry and carbon isotope clines (Figure 1, Table 1). Ventral coloration
355 differed on either side of the mountains in Mongolia (Table 1). In the *rustica-gutturalis* transect
356 in China, the cline for color was narrow but the center was displaced to the east of the other
357 clines (Figure 1, S1, Table 1). There may thus be some differential introgression of plumage

358 color between *rustica* and *gutturalis*, although differences in color were small because both
359 subspecies have mostly white ventral plumage (Figure S1).

360 Clines for wing pointedness were narrow and coincident with the ancestry and carbon
361 isotope clines in the two *rustica-tytleri* transects, but did not vary across the *rustica-gutturalis*
362 transect (Table S1). Tail streamer length, throat color, wing convexity, and wing length either did
363 not vary clinally or exhibited very wide clines (Table S1). Thus, carbon isotope value (reflecting
364 different wintering grounds) was the only trait consistently associated with genetic ancestry and
365 limited hybridization across the *rustica* pairs. This result supports our prediction that narrow
366 hybrid zones are associated with migratory divides. The convergent geographic locations of
367 ancestry and migratory clines strongly suggests that differences in wintering grounds are driven
368 by divergent migratory routes around the Tibetan Plateau (Figure 1).

369

370 Geographic clines- tytleri/gutturalis pair: There was extensive admixture and no clear
371 association between genetic ancestry and phenotype across the three *tytleri-gutturalis* transects.
372 Ancestry clines were wide, with only the cline in China narrower than the neutral expectation
373 (Table 1, Figure 1 E-F). Furthermore, there was no clinal variation in ancestry across Mongolia,
374 indicative of homogenous admixture (Figure 1F, S1). There was also no clinal variation in
375 carbon isotope values across any of the three *tytleri-gutturalis* transects (Figure 1, Table 1). The
376 only transect with a ventral color cline narrower than the neutral expectation was in China, where
377 the cline was concordant with ancestry (Table 1). As with the *rustica* pairs, morphometric traits
378 did not vary clinally across the transects (Table S1). These analyses reveal large geographic
379 regions of nearly homogenous admixture and little phenotypic differentiation between *tytleri* and

380 *gutturalis*, in contrast to the narrow hybrid zones that coincided with migratory phenotype and,
381 to some extent, color, in the *rustica* migratory divides.

382

383 ***Prediction 2: Migratory phenotype is associated with genetic differentiation***

384 We predicted that if migratory divides are important reproductive barriers, differences in
385 migratory behavior would explain large proportions of among-individual genome-wide variance
386 relative to other divergent traits within migratory divides. The combined effects of color,
387 migratory phenotype, and geographic location explained 34% of among-individual genetic
388 variance (PC1 and PC2) in the Russian *rustica-tytleri* transect (Figure 3A). The combination of
389 geography and migratory phenotype explained 30% of genetic variance between *rustica-tytleri* in
390 Mongolia (Figure 3C) and 23% between *rustica-gutturalis* in China (Figure 3F). Migratory
391 phenotype explained statistically significant proportions of genetic variance when controlling for
392 the effects of color and geography in the *rustica-tytleri* transect in Russia and the *rustica-*
393 *gutturalis* transect in China (Table S2). Color explained significant proportions of genetic
394 variance in the two *rustica-tytleri* transects when controlling for geography and migratory
395 phenotype, but not in the *rustica-gutturalis* transect in China (Table S2). Overall, the
396 combination of migratory phenotype and geography explained larger proportions of variance
397 than did geography and color in two of the three *rustica* transects. The combination of all three
398 factors explained the largest proportion of variance in the *rustica-tytleri* transect in Siberia
399 (Figure 3).

400 In the three *tytleri-gutturalis* transects without migratory divides, migratory phenotype
401 explained a maximum of 2% of among-individual genetic variance when combined with
402 geography (Figure 3 B, D, F, Table S2), consistent with no clear migratory divide in these

403 regions. Geography and color explained comparatively larger proportions of genetic variance (2-
404 28%, Figure 3, Table S2).

405 We visualized these individual-level associations by plotting frequency distributions of
406 genotypes and phenotypes. The two subspecies pairs with migratory divides exhibited bimodal
407 distributions of carbon isotope values coinciding with bimodal distributions of genotypes, with
408 the rare hybrids expressing trait values that spanned the full parental range (Figure 4A, B). By
409 contrast, carbon isotope distributions were unimodal between all *tytleri* and *gutturalis*
410 populations, and hybrid genotypes were common (Figure 4C). Distributions of ventral color
411 showed a different pattern: *rustica* and *gutturalis* have white ventral plumage, whereas *tytleri* is
412 dark brown, resulting in bimodal color distributions between *rustica-tytleri* and *tytleri-gutturalis*
413 (Fig 4E, F) and a unimodal distribution between *rustica-gutturalis* (Fig 4D). Color distributions
414 did not match genotype distributions: there was limited hybridization between *rustica-gutturalis*
415 despite similar ventral color, and extensive hybridization between *tytleri-gutturalis* despite
416 different ventral color.

417

418 ***Prediction 3: Assortative mating is based on migratory phenotype***

419 We found that divergent migratory phenotypes, and, to a lesser extent, divergent color were
420 associated with limited hybridization and comparatively large genome-wide variance. Lastly, we
421 predicted that if migratory behavior *per se* acts as a barrier to reproduction, we would observe
422 assortative mating by migratory phenotype in hybrid zones with migratory divides. We assessed
423 the contribution of migratory phenotype to premating reproductive isolation using social pairing
424 data across three transects: the *rustica-tytleri* hybrid zone in Russia, the *rustica-gutturalis* hybrid

425 zone in China, and the *tytleri-gutturalis* transect in China (Figure 1). The first two transects have
426 migratory divides, while the third does not.

427

428 Phenotype networks: Phenotype networks indicated assortative mating by genotype across all
429 three transects (Figure 5: black lines connecting male and female genotypes; *rustica-gutturalis*
430 $r_{\text{genotype}} = 0.82$; *rustica-tytleri* $r_{\text{genotype}} = 0.48$; *tytleri-gutturalis* $r_{\text{genotype}} = 0.50$). In the two
431 transects with migratory divides, carbon isotope values were correlated within pairs (Figure 5A,
432 B, gray lines). An individual's genotype also correlated with its mate's carbon isotope value
433 (Figure 5A, B, black lines; *rustica-gutturalis*: $r_{\text{carbon}} = 0.56$ and 0.36 ; *rustica-tytleri*: $r_{\text{carbon}} = 0.56$
434 and 0.47), suggesting that overwintering grounds are an important basis for assortative mating.
435 Carbon values were not associated with assortative mating in the transect without a migratory
436 divide (*tytleri-gutturalis*, Figure 5C).

437 Ventral coloration was correlated with mate's genotype in all three transects (*rustica-*
438 *gutturalis*: $r_{\text{color}} = 0.35$, *rustica-tytleri*: $r_{\text{color}} = 0.58$, *tytleri-gutturalis*: $r_{\text{color}} = 0.38$, Figure 4). The
439 correlations for color were weaker than those for carbon isotopes in the *rustica-gutturalis*
440 transect (Figure 5A) and similar in the *rustica-tytleri* transect (Figure 5B). We interpret this as
441 evidence for migratory behavior and, to a lesser extent, coloration, in mediating broad patterns of
442 assortative mating across hybrid zones with migratory divides. However, genotype and phenotype
443 also correlated with geographic location in all three transects (Figure 5). These correlations
444 reflect geographic variation in the frequencies of different genotypes and phenotypes (Figure 1),
445 and suggest that broad patterns of assortative mating may be due in part to variation in the
446 availability of homo- vs. heterotypic individuals as mates.

447

448 Reproductive isolation index: Applying an index of premating reproductive isolation (RI)
449 allowed us to control for variation in available mates at a fine geographic scale (Figure S3). In
450 the *rustica-tyleri* transect in Russia, both parentals and hybrids co-occurred in several
451 populations (Figure S3A). Assortative mating by genotype was comparatively weak in these
452 populations (Figure S3A). However, in all populations where both parental forms coexisted,
453 there was evidence for assortative mating by migratory phenotype (average RI= 0.28). Isolation
454 was strongest among *rustica* individuals (RI= 0.52); that is, individuals assigned *rustica*
455 migratory phenotypes were >50% more likely to pair with each other than with a *tyleri*
456 migratory phenotype. Assortative mating by color was less consistent among populations (Figure
457 S3A). This result suggests a central role for divergent migratory behavior in mediating premating
458 reproductive isolation between *rustica* and *tyleri*.

459 There was some assortative mating by genotype in the *rustica-gutturalis* transect in China
460 (average RI= 0.14, Figure S3B). However, this was due to the absence of parentals from the
461 hybrid zone center and consequent high pairing frequency among hybrids (“conspecific”
462 matings); indeed, there was no population in which parental *rustica* and *gutturalis* co-occurred
463 (Figure S3B). There was some weak assortative mating by migratory phenotype in the hybrid
464 zone center (Figure S3B), but mating was otherwise random based on phenotype.

465 In contrast to the two migratory divides, we did not detect assortative mating across the
466 *tyleri-gutturalis* transect in China. Genotype frequencies were fairly homogeneously admixed
467 across the transect, and both migratory phenotype and color varied little, making the question of
468 premating isolation less relevant (Figure S3C). Taken together, our measurement of premating
469 barriers suggests stronger assortative mating by migratory phenotype than color in both
470 migratory divides. However, the distributions of parental vs. hybrid genotypes, and hence

471 potential mates, varied substantially. The mechanism by which migratory divides contribute to
472 reproductive barriers may therefore differ between subspecies pairs (Figure S3).

473

474 **Discussion**

475 We tested the hypothesis that migratory divides are broadly important to the maintenance of
476 reproductive barriers between barn swallow subspecies by sampling comprehensively across
477 multiple contact zones. Our analyses collectively suggest that 1) there was less hybridization
478 across transects with migratory divides than across transects without migratory divides; 2)
479 divergent migratory behavior explained large proportions of genetic variance relative to other
480 traits within migratory divides; and 3) divergent migratory behavior *per se* contributed to
481 premating reproductive barriers. Further, geographic coincidence between migratory divides and
482 narrow hybrid zones supports a longstanding hypothesis (Irwin & Irwin 2005) that divergent
483 migratory routes around the Tibetan Plateau maintain range boundaries in Siberian and central
484 Asian avifauna.

485 Many birds that breed in Asia circumnavigate the inhospitable Tibetan Plateau to the east
486 or west en route to wintering grounds in south Asia or Africa (Irwin & Irwin 2005). By sampling
487 most of the Asian range of the barn swallow, we found multiple migratory divides centered at the
488 same longitude (~100 degrees) but at different latitudes and between different subspecies pairs.
489 These narrow hybrid zones occurred across regions with no obvious ecological gradients or
490 barriers to dispersal, suggesting isolation is not due to divergent ecological selection during the
491 breeding season. Instead, the striking coincidence in width and geographic locations of the
492 hybrid zones, and the similar proportions of backcrosses in each zone (Figure S2), suggest that
493 hybrid zones have independently settled in regions where selection against hybrids is

494 symmetrical (Price 2008) or costs of long-distance migration are minimized (Toews 2017). Such
495 observations implicate a major barrier that drives both the location and extent of hybridization
496 across a broad geographic region. Limited hybridization in these areas is the pattern we would
497 predict if the Tibetan Plateau shapes differences in migratory behavior and contributes to the
498 maintenance of species boundaries.

499 Social pairing data further suggest that assortative mating by migratory phenotype may
500 be an important premating barrier to hybridization between *rustica* and *tytleri*. However,
501 although migratory phenotype explained large proportions of genetic variance, premating
502 isolation was weaker between *rustica* and *gutturialis* in China, likely due to the absence of
503 parental individuals in the center of the hybrid zone. In birds, it has been proposed that premating
504 barriers often arise early in divergence, with postmating barriers and reinforcement appearing
505 later via selection against unfit hybrids (Price 2008). Different isolating mechanisms operating
506 within the two migratory divides may reflect different lengths of time since secondary contact, as
507 well as contributions of other variables, such as competitive exclusion or unmeasured ecological
508 factors, to isolation. Intrinsic postmating barriers are unlikely given shallow divergence (Zink *et*
509 *al.* 2006; Smith *et al.* 2018), presence of backcrosses in all hybrid zones, and the absence of
510 fixed differences between any subspecies pair. It remains possible that as-yet-undetected loci are
511 associated with divergent migratory behaviors and cause intrinsic genetic incompatibilities in
512 hybrids. However, many other migratory divides lack evidence for hybrid unfitness or genetic
513 differentiation associated with migratory phenotypes (Davis *et al.* 2006; Liedvogel *et al.* 2014;
514 Ramos *et al.* 2017; Toews *et al.* 2017). It is therefore more likely that assortative mating and
515 extrinsic selection against hybridization maintain narrow hybrid zones at migratory divides,

516 although we cannot assess the relative importance of pre- vs. postmating barriers with our
517 current data.

518 Here we present evidence for a central role of divergent migratory behavior in the
519 maintenance of reproductive boundaries across replicated hybrid zones, supporting a
520 longstanding but rarely evaluated hypothesis that migratory behavior can be an important engine
521 of speciation. Future work studying hybrid fitness will further clarify the mechanisms by which
522 reproductive isolation is maintained within migratory divides.

523

524 **Acknowledgements**

525 We are grateful to the State Darwin Museum in Moscow, Hainan Normal University, National
526 University of Mongolia, the Mongolian Ornithological Society, and the Japan Bird Research
527 Association for sponsoring our research. Work was conducted in accordance with University of
528 Colorado IACUC protocol #1303. Many people assisted with fieldwork, including Caroline
529 Glidden, Rachel Lock, Yulia Sheina, Nikolai Markov, Gennady Bachurin, Olga Zayatseva, Elena
530 Shnayder, Unurjargal Enkhbat, Bayanmunkh Dashnyam, Davaadorj Enkhbayar, Wataru
531 Kitamura, Takashi Tanioka, and Yuta Inaguma. Brittany Jenkins prepared the genomic libraries.
532 Dai Shizuka advised on the phenotype networks. We thank Amanda Hund, Bruce Lyon, Trevor
533 Price, Scott Taylor, and the Safran and Taylor labs at the University of Colorado for feedback on
534 the manuscript. This project was funded by NSF-CAREER grant DEB-1149942 to RJS and the
535 National Geographic Society Committee on Research and Exploration grant to ESCS.

536

537

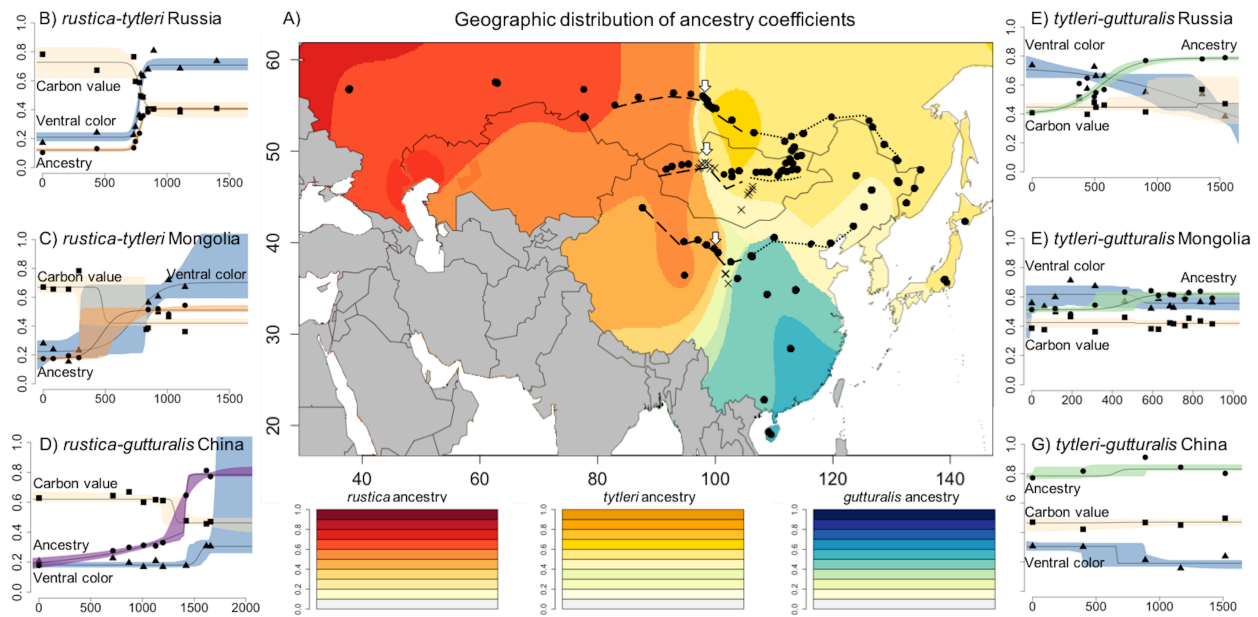
538

539 **References**

- 540
- 541 Badyaev, A.V. & Young, R.L. (2004). Complexity and integration in sexual ornamentation: an
542 example with carotenoid and melanin plumage pigmentation. *J. Evol. Biol.*, 17, 1317–
543 1327.
- 544 Barton, N.H. & Gale, K.S. (1993). Genetic Analysis of Hybrid Zones. In: *Hybrid Zones and the*
545 *Evolutionary Process*. Oxford University Press, pp. 13–45.
- 546 Bearhop, S., Fiedler, W., Furness, R.W., Votier, S.C., Waldron, S., Newton, J., *et al.* (2005).
547 Assortative mating as a mechanism for rapid evolution of a migratory divide. *Science*,
548 310, 502–504.
- 549 Berthold, P., Helbig, A.J., Mohr, G. & Querner, U. (1992). Rapid microevolution of migratory
550 behaviour in a wild bird species. *Nature*, 360, 668–670.
- 551 Brelsford, A. & Irwin, D.E. (2009). Incipient speciation despite little assortative mating: the
552 yellow-rumped warbler hybrid zone. *Evolution*, 63, 3050–3060.
- 553 Caye, K., Deist, T.M., Martins, H., Michel, O. & François, O. (2016). TESS3: fast inference of
554 spatial population structure and genome scans for selection. *Mol. Ecol. Resour.*, 16, 540–
555 548.
- 556 Davis, L.A., Roalson, E.H., Cornell, K.L., Mcclanahan, K.D. & Webster, M.S. (2006). Genetic
557 divergence and migration patterns in a North American passerine bird: implications for
558 evolution and conservation. *Mol. Ecol.*, 15, 2141–2152.
- 559 Delmore, K.E. & Irwin, D.E. (2014). Hybrid songbirds employ intermediate routes in a
560 migratory divide. *Ecol. Lett.*, 17, 1211–1218.
- 561 Delmore, K.E., Toews, D.P., Germain, R.R., Owens, G.L. & Irwin, D.E. (2016). The Genetics of
562 Seasonal Migration and Plumage Color. *Curr. Biol.*, 26, 2167–2173.
- 563 Derryberry, E.P., Derryberry, G.E., Maley, J.M. & Brumfield, R.T. (2014). HZAR: hybrid zone
564 analysis using an R software package. *Mol. Ecol. Resour.*, 14, 652–663.
- 565 Dor, R., Safran, R.J., Sheldon, F.H., Winkler, D.W. & Lovette, I.J. (2010). Phylogeny of the
566 genus *Hirundo* and the Barn Swallow subspecies complex. *Mol. Phylogenet. Evol.*, 56,
567 409–418.
- 568 Epskamp, S., Cramer, A.O., Waldorp, L.J., Schmittmann, V.D. & Borsboom, D. (2012). qgraph:
569 Network visualizations of relationships in psychometric data. *J. Stat. Softw.*, 48, 1–18.
- 570 Gay, L., Crochet, P.-A., Bell, D.A. & Lenormand, T. (2008). Comparing clines on molecular and
571 phenotypic traits in hybrid zones: a window on tension zone models. *Evolution*, 62,
572 2789–2806.
- 573 Gompert, Z. & Buerkle, C.A. (2016). What, if anything, are hybrids: enduring truths and
574 challenges associated with population structure and gene flow. *Evol. Appl.*, 9, 909–923.
- 575 Goslee, S.C. & Urban, D.L. (2007). The ecodist package for dissimilarity-based analysis of
576 ecological data. *J. Stat. Softw.*, 22, 1–19.
- 577 Helbig, A. (1996). Genetic basis, mode of inheritance and evolutionary changes of migratory
578 directions in palaeartic warblers (Aves: Sylviidae). *J. Exp. Biol.*, 199, 49–55.
- 579 Helbig, A.J. (1991). Inheritance of migratory direction in a bird species: a cross-breeding
580 experiment with SE- and SW-migrating blackcaps (*Sylvia atricapilla*). *Behav. Ecol.*
581 *Sociobiol.*, 28, 9–12.
- 582 Hubbard, J.K., Jenkins, B.R. & Safran, R.J. (2015). Quantitative genetics of plumage color:
583 lifetime effects of early nest environment on a colorful sexual signal. *Ecol. Evol.*, 5,
584 3436–3449.

- 585 Irwin, D.E. & Irwin, J.H. (2005). Siberian migratory divides. In: *Birds of Two Worlds: The*
586 *Ecology and Evolution of Migration* (eds. Greenberg, R. & Marra, P.P.). Johns Hopkins
587 University Press, Baltimore, pp. 27–40.
- 588 Kelly, J.F. (2000). Stable isotopes of carbon and nitrogen in the study of avian and mammalian
589 trophic ecology. *Can. J. Zool.*, 78, 1–27.
- 590 Li, H. & Durbin, R. (2009). Fast and accurate short read alignment with Burrows–Wheeler
591 transform. *Bioinformatics*, 25, 1754–1760.
- 592 Li, H., Handsaker, B., Wysoker, A., Fennell, T., Ruan, J., Homer, N., *et al.* (2009). The sequence
593 alignment/map format and SAMtools. *Bioinformatics*, 25, 2078–2079.
- 594 Liedvogel, M., Larson, K.W., Lundberg, M., Gursoy, A., Wassenaar, L.I., Hobson, K.A., *et al.*
595 (2014). No evidence for assortative mating within a willow warbler migratory divide.
596 *Front. Zool.*, 11, 52.
- 597 Lockwood, R., Swaddle, J.P. & Rayner, J.M.V. (1998). Avian Wingtip Shape Reconsidered:
598 Wingtip Shape Indices and Morphological Adaptations to Migration. *J. Avian Biol.*, 29,
599 273.
- 600 Lundberg, M., Liedvogel, M., Larson, K., Sigeman, H., Grahn, M., Wright, A., *et al.* (2017).
601 Genetic differences between willow warbler migratory phenotypes are few and cluster in
602 large haplotype blocks. *Evol. Lett.*, 1, 155–168.
- 603 Oksanen, J., Blanchet, F.G., Kindt, R., Legendre, P., Minchin, P.R., O’Hara, R.B., *et al.* (2013).
604 Package ‘vegan.’ *Community Ecol. Package Version*, 2.
- 605 Paradis, E., Baillie, S.R., Sutherland, W.J. & Gregory, R.D. (1998). Patterns of natal and
606 breeding dispersal in birds. *J. Anim. Ecol.*, 67, 518–536.
- 607 Price, T. (2008). *Speciation in Birds*. Roberts and Co.
- 608 Raj, A., Stephens, M. & Pritchard, J.K. (2014). fastSTRUCTURE: variational inference of
609 population structure in large SNP data sets. *Genetics*, 197, 573–589.
- 610 Ramos, J.S.L., Delmore, K.E. & Liedvogel, M. (2017). Candidate genes for migration do not
611 distinguish migratory and non-migratory birds. *J. Comp. Physiol. A*, 203, 383–397.
- 612 Reverter, A. & Chan, E.K. (2008). Combining partial correlation and an information theory
613 approach to the reversed engineering of gene co-expression networks. *Bioinformatics*, 24,
614 2491–2497.
- 615 Rolshausen, G., Segelbacher, G., Hobson, K.A. & Schaefer, H.M. (2009). Contemporary
616 evolution of reproductive isolation and phenotypic divergence in sympatry along a
617 migratory divide. *Curr. Biol.*, 19, 2097–2101.
- 618 Ruegg, K. (2008). Genetic, morphological, and ecological characterization of a hybrid zone that
619 spans a migratory divide. *Evolution*, 62, 452–466.
- 620 Ruegg, K., Anderson, E.C. & Slabbekoorn, H. (2012). Differences in timing of migration and
621 response to sexual signalling drive asymmetric hybridization across a migratory divide. *J.*
622 *Evol. Biol.*, 25, 1741–1750.
- 623 Safran, R.J. & McGraw, K.J. (2004). Plumage coloration, not length or symmetry of tail-
624 streamers, is a sexually selected trait in North American barn swallows. *Behav. Ecol.*, 15,
625 455–461.
- 626 Safran, R.J., Scordato, E.S.C., Wilkins, M.R., Hubbard, J.K., Jenkins, B.R., Albrecht, T., *et al.*
627 (2016). Genome-wide differentiation in closely related populations: the roles of selection
628 and geographic isolation. *Mol. Ecol.*, 25, 3865–3883.
- 629 Scordato, E.S. & Safran, R.J. (2014). Geographic variation in sexual selection and implications
630 for speciation in the Barn Swallow. *Avian Res.*, 5, 1–13.

- 631 Scordato, E.S.C., Wilkins, M.R., Semenov, G., Rubtsov, A.S., Kane, N.C. & Safran, R.J. (2017).
632 Genomic variation across two barn swallow hybrid zones reveals traits associated with
633 divergence in sympatry and allopatry. *Mol. Ecol.*, 26, 5676–5691.
- 634 Shafer, A.B.A. & Wolf, J.B.W. (2013). Widespread evidence for incipient ecological speciation:
635 a meta-analysis of isolation-by-ecology. *Ecol. Lett.*, 16, 940–950.
- 636 Shizuka, D. & Farine, D.R. (2016). Measuring the robustness of network community structure
637 using assortativity. *Anim. Behav.*, 112, 237–246.
- 638 Smith, C.C.R., Flaxman, S.M., Scordato, E.S.C., Kane, N.C., Hund, A.K., Sheta, B.M., *et al.*
639 (2018). Demographic inference in barn swallows using whole-genome data shows signal
640 for bottleneck and subspecies differentiation during the Holocene. *Mol. Ecol.*, 1–13.
- 641 Still, C.J., Berry, J.A., Collatz, G.J. & DeFries, R.S. (2003). Global distribution of C3 and C4
642 vegetation: carbon cycle implications. *Glob. Biogeochem. Cycles*, 17.
- 643 Sullivan, B.L., Wood, C.L., Iliff, M.J., Bonney, R.E., Fink, D. & Kelling, S. (2009). eBird: A
644 citizen-based bird observation network in the biological sciences. *Biol. Conserv.*, 142,
645 2282–2292.
- 646 Szymura, J.M. & Barton, N.H. (1986). Genetic analysis of a hybrid zone between the fire-bellied
647 toads, *Bombina bombina* and *B. variegata*, near Cracow in southern Poland. *Evolution*,
648 1141–1159.
- 649 Taylor, R.S. & Friesen, V.L. (2017). The role of allochryony in speciation. *Mol. Ecol.*, 26, 3330–
650 3342.
- 651 Toews, D.P.L. (2017). Habitat suitability and the constraints of migration in New World
652 warblers. *J. Avian Biol.*, 48, 1614–1623.
- 653 Toews, D.P.L., Delmore, K.E., Osmond, M.M., Taylor, P.D. & Irwin, D.E. (2017). Migratory
654 orientation in a narrow avian hybrid zone. *PeerJ*, 5, e3201.
- 655 Turbek, S.P., Scordato, E.S.C. & Safran, R.J. (2018). The Role of Seasonal Migration in
656 Population Divergence and Reproductive Isolation. *Trends Ecol. Evol.*, 33, 164–175.
- 657 Turner, A. (2010). *The Barn Swallow*. Bloomsbury Publishing.
- 658 Wang, I.J. (2013). Examining the full effects of landscape heterogeneity on spatial genetic
659 variation: a multiple matrix regression approach for quantifying geographic and
660 ecological isolation: special section. *Evolution*, 67, 3403–3411.
- 661 Watson-Haigh, N.S., Kadarmideen, H.N. & Reverter, A. (2009). PCIT: an R package for
662 weighted gene co-expression networks based on partial correlation and information
663 theory approaches. *Bioinformatics*, 26, 411–413.
- 664 Wilkins, M.R., Shizuka, D., Joseph, M.B., Hubbard, J.K. & Safran, R.J. (2015). Multimodal
665 signalling in the North American barn swallow: a phenotype network approach. *Proc. R.*
666 *Soc. B Biol. Sci.*, 282, 20151574.
- 667 Zink, R.M., Pavlova, A., Rohwer, S. & Drovetski, S.V. (2006). Barn swallows before barns:
668 population histories and intercontinental colonization. *Proc. R. Soc. B Biol. Sci.*, 273,
669 1245–1251.
- 670
- 671
- 672
- 673



674

675 **Figure 1: Geographic variation in ancestry coefficients and phenotypes across Asia. A)**

676 ancestry coefficients derived from spatially explicit modeling of >12,000 SNPs. Darker colors

677 reflect more parental-like ancestry (red=*rustica*, gold=*tytleri*, blue=*gutturalis*; see legend). Paler

678 colors reflect regions with more admixed individuals. Points indicate sampling locations. X's are

679 surveyed regions with no breeding barn swallows. Dashed lines show *rustica* transects used in

680 geographic cline analysis (left panels) and dotted lines show *tytleri-gutturalis* transects (right

681 panels). All cline plots show standardized trait values (y-axis) plotted against distance from the

682 westernmost point of the transect (x-axis). **Left panels:** clines for genetic ancestry (orange:

683 *rustica-tytleri*; purple: *rustica-gutturalis*), carbon value (tan clines), and ventral coloration (blue

684 clines) across the three western sampling transects (B: Russia; C: Mongolia; D: China). Clines

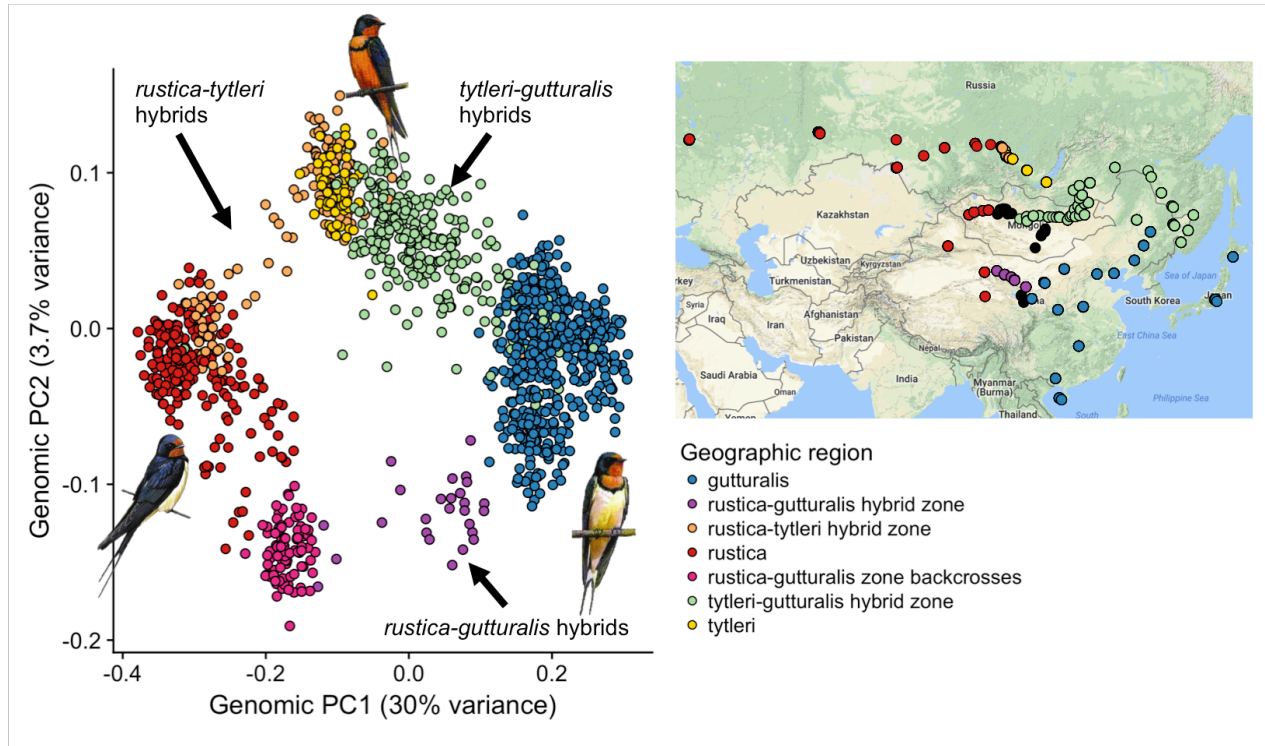
685 for carbon value and ancestry are steep and coincident across all three contact zones, and cline

686 centers all occur at 98-100 degrees longitude (centers marked on map with white arrows). **Right**

687 **panels:** geographic clines for ancestry (green clines: *tytleri-gutturalis*), carbon value (tan clines),

688 and ventral coloration (blue clines) across the three eastern sampling transects (E: Russia; F:

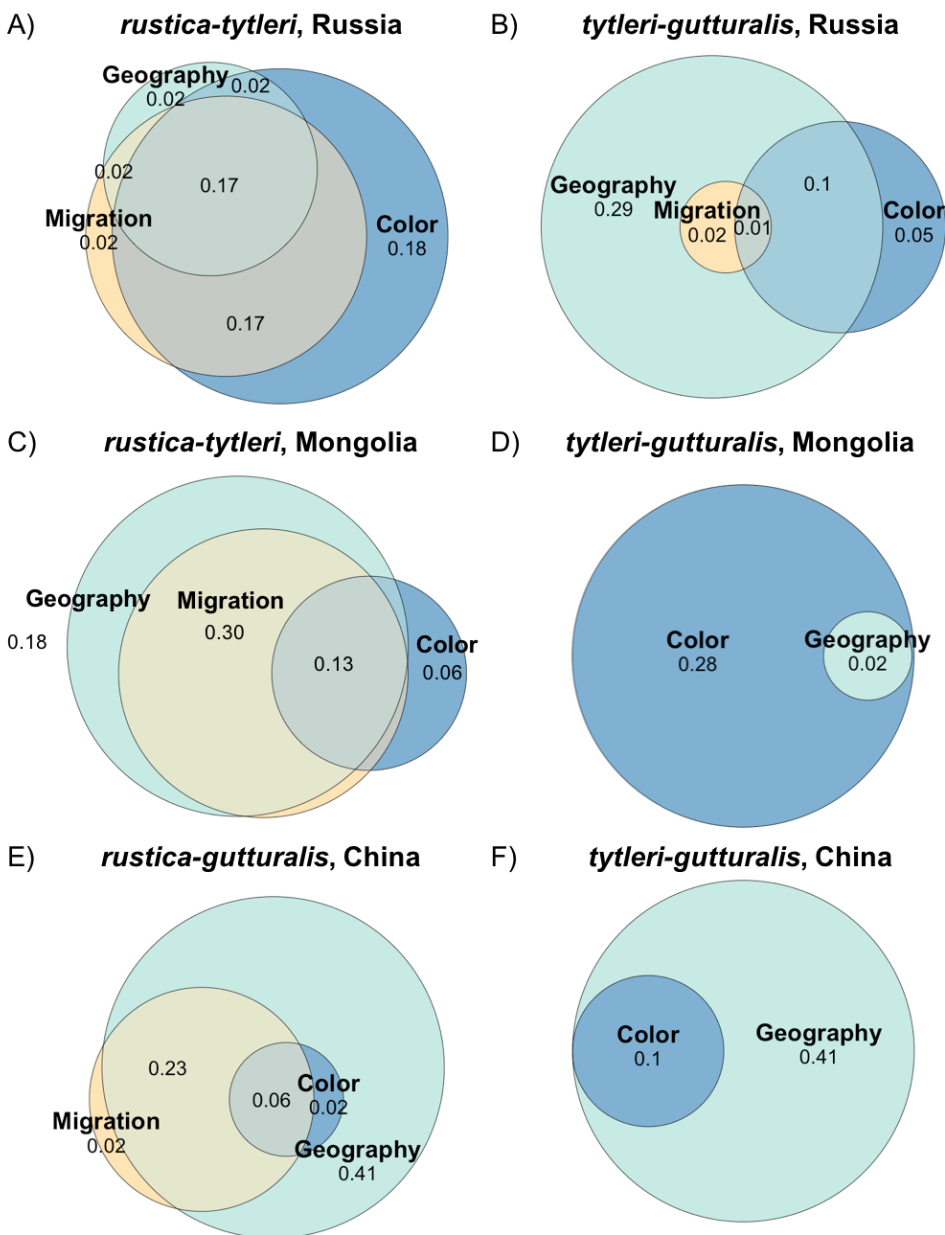
689 Mongolia; G: China). Ancestry clines are shallow and broad, and there is no variation in isotope
690 values and little variation in ventral color across the transects.
691



692
693

694 **Figure 2: The first two principal components from a PCA of the genetic covariance matrix**
695 **of all individual birds.** Point colors correspond to geographic sampling regions, as indicated in
696 the legend and on the inset map. The PCA generally recapitulates geography and recovers three
697 parental clusters (*rustica* in red, *tyleri* in gold, and *gutturalis* in blue). Points connecting these
698 clusters correspond to admixed individuals (labeled arrows). The pink cluster at PC1= -0.2 are
699 birds captured in the *rustica-gutturalis* hybrid zone (purple points on map) that appear to be late
700 generation backcrosses to *rustica* and form their own discrete genetic cluster. Drawings show
701 typical phenotype for each of the three parental subspecies. Inset: map of sampling locations
702 with points colored corresponding to geography in the main figure legend. Black points are
703 sampled areas where no birds were found to be breeding. Drawings courtesy of Hilary Burns.
704

705



706

707

Figure 3: Genomic variance (PC1 and PC2) partitioned among traits related to migratory

708

phenotype (carbon value), sexual signaling (ventral color), and geographic location of sampling

709

(latitude and longitude). Variance is shown as adjusted R² values. Variance is partitioned among

710

the subsets of individuals occurring along each of the six transects through regions of

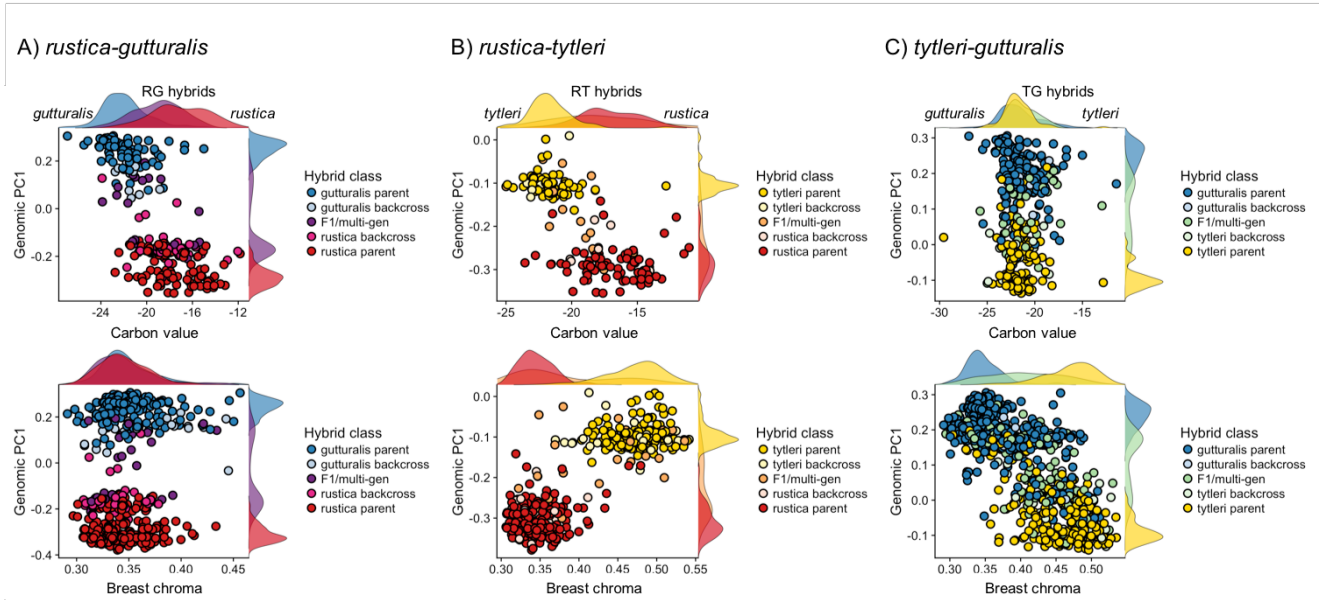
711

hybridization shown in Figure 1. Each row shows a transect with a migratory divide on the left

712

and the parallel transect (same latitude, different longitude) without a migratory divide on the

713 right. Overlapping regions between circles show the amount of genetic variance explained by the
714 combined effects of those variables; for example, the combination of migratory phenotype, color,
715 and geographic location explains 17% of the genetic variance in the *rustica-tytleri* transect in
716 Russia (A) and the combination of migratory phenotype and geographic location explains 30%
717 of the genetic variance in the *rustica-tytleri* transect in Mongolia (C). Note that migratory
718 phenotype explains no genetic variance in the *tytleri-gutturalis* transects in Mongolia and China.
719

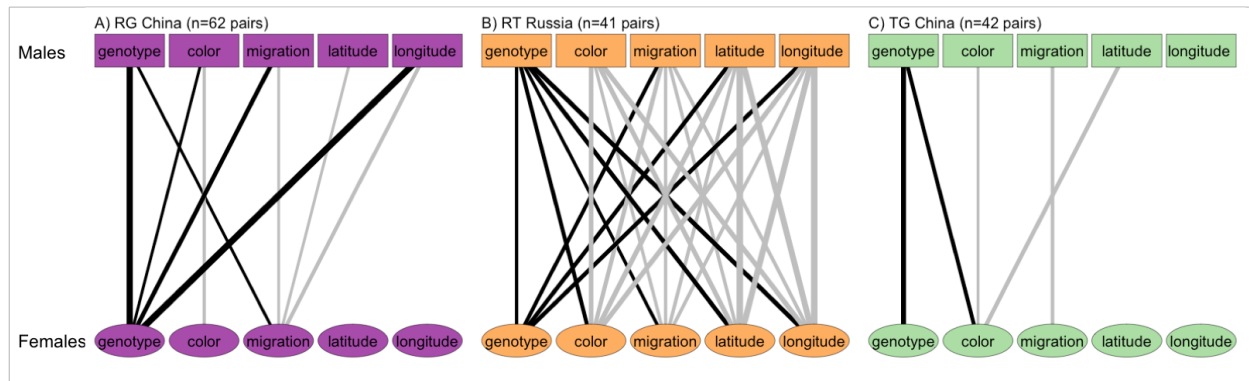


720
721

722 **Figure 3: Distribution of genotypes and phenotypes between each of the three subspecies**
723 **pairs.** Each point is an individual bird, with points colored by hybrid class assignment (parental,
724 backcross, or F1/multigenerational hybrid). Genomic PC1 score is on the y-axis of all plots. Y-
725 axis density plots show the distribution of genomic ancestry for parentals and hybrids
726 (backcrosses, F1, multigenerational hybrids combined) between each subspecies pair
727 (red=*rustica*, blue=*gutturalis*, yellow=*tytleri*). Note clear bimodal distributions with few
728 intermediates between *rustica-gutturalis* (purple) and *rustica-tytleri* (orange), but a broad range
729 of genomically intermediate individuals between *tytleri* and *gutturalis* (green). There is also a
730 separate peak in genomic PC scores in the *rustica-gutturalis* contact zone (A, purple peak on y-
731 axis) comprised of late generation back-crossed individuals. **Top row:** Genomic PC1 score is
732 plotted against carbon value(x-axis). There were generally bimodal distributions in carbon values
733 between parental individuals in the *rustica-gutturalis* and *rustica-tytleri* pairs, corresponding to
734 bimodal distributions of parental genotypes. In the *rustica-gutturalis* hybrid zone (A, purple),
735 hybrid genotypes and carbon isotope ratios were more similar to parental *rustica*. In the *rustica-*

736 *tyleri* hybrid zone (B, orange), hybrid genotypes and carbon isotope ratios were more similar to
737 *tyleri*, but F1/multigenerational hybrids had isotope ratios spanning the full parental range. In
738 the *tyleri-gutturalis* hybrid zones (C, green), there were no differences in isotope ratios between
739 parentals and hybrids **Bottom row:** Genomic PC score is plotted against breast chroma (x-axis).
740 A) There are few hybrids between *rustica* and *gutturalis* despite similar parental ventral color. B)
741 In the *rustica-tyleri* and C) *tyleri-gutturalis* zones, we find bimodal distributions in ventral
742 color. There are few hybrids between *rustica-tyleri* (B, orange) but many hybrids between
743 *tyleri-gutturalis* (C, green), despite differences in ventral color.
744

745



746

747

748 **Figure 5: Bipartite phenotype networks showing traits associated with assortative mating**

749 **across three transects.** Black lines show characteristics that predict the ancestry of an

750 individual's social mate (the traits most relevant for reducing gene flow). Gray lines show traits

751 correlated within pairs. Line width reflects the strength of the correlation. Squares (top row) are

752 males. Circles (bottom row) are females. In the two migratory divides (A and B), an individual's

753 genotype is correlated with the migratory phenotype (carbon value) and ventral coloration of its

754 social mate (black lines between traits and genotypes). There is also strong assortative mating by

755 genotype. In the *tyleri-gutturalis* transect in China (C), there is assortative mating by genotype,

756 and ventral coloration is associated with social mate's genotype. In the migratory divides (A and

757 B) there are also strong correlations between geographic location and genotype, indicating

758 geographic variation in the distribution of available mates.

759

760 **Table 1: Best-fit geographic cline models for each trait and each transect.** Boldfaced clines
 761 are those that have centers coincident with the ancestry cline. Starred widths are narrower than
 762 expected under a neutral diffusion model assuming a dispersal distance of 42 km and a hybrid
 763 zone age older than 20 years. The § symbol shows clines that are wider than expected with a
 764 dispersal distance of 42km, but narrower than expected if dispersal is 100km and clines are older
 765 than 20 years. Italicized clines show no statistically significant variation in trait values across the
 766 transect and are consequently poorly described by cline models. Carbon clines coincide with
 767 ancestry in the three *rustica* transects (top three rows) but not in the *tytleri-gutturalis* transects
 768 (bottom three rows). Cline center units are kilometers from the westernmost transect point.

769

Transect	Ancestry Center	Ancestry width (km)	Carbon value center	Carbon value width (km)	Breast chroma center	Breast chroma width (km)
RG-China	1405.39 (1286.03-1405.39)	51.55* (51.55-416.46)	1307.65 (1199.6-1412.04)	43.16 * (0.22-496.16)	1541.49 (1454.64-1999.83)	96.97 * (1.19-539.04)
RT-Mongolia	471.56 (365.65-563.93)	267.97 § (93.06-463.12)	476.17 (291.02-827.37)	44.79* (0.02-227.09)	736.02 (551.38-962.71)	425.3 § (64.2-1698.19)
RT-Russia	781.07 (771.11-787.88)	87.75* (72.78-114)	775.63 (753.85-799.19)	102.88* (51.58-181.19)	774.74 (766.85-783.11)	70.0* (47.58-102.77)
TG-China	659.35 (345.45-871.81)	118.18* (4.84-256.9)	<i>668.16</i> (<i>364-1322.56</i>)	<i>384.63</i> (<i>32.09-2008.83</i>)	662.26 (387.93-909.19)	2.35* (0-1167.15)
TG-Mongolia	<i>484.38</i> (<i>315.33-532.5</i>)	<i>201.05</i> (<i>0.45-340.66</i>)	<i>510.79</i> (<i>390.41-522.11</i>)	<i>12.61</i> (<i>0.14-172.41</i>)	<i>526.76</i> (<i>31.7-1458.11</i>)	<i>59.28</i> (<i>0-238.12</i>)
TG-Russia	544.34 (505.88-586.1)	555.59 (450.56-693.96)	<i>1324.01</i> (<i>906.2-1444.22</i>)	6.27 (0-74.94)	1324.91 (512.67-1997.59)	1653.72 (258.18-2029.86)

770

771